e_g-level splitting in a layered perovskite manganite as revealed by charge modulation spectroscopy

Masao Nakamura,[1,*] Masashi Kawasaki,[1,2] and Yoshinori Tokura[1,2]

[1]*Cross-Correlated Materials Research Group (CMRG) and Correlated Electron Research Group (CERG), Advanced Science Institute, RIKEN, Wako 351-0198, Japan*

[2]*Department of Applied Physics and Quantum Phase Electronics Center (QPEC), University of Tokyo, Tokyo 113-8656, Japan*

(Received 26 March 2012; revised manuscript received 29 August 2012; published 18 September 2012)

An orbital degree of freedom in Mott insulators gives strong impact on their phase transitions induced by the band-filling control or carrier doping. We have investigated the effect of electrostatic carrier doping on the electronic spectra for a layered Mott insulator Sr_2MnO_4 to reveal orbital-specific optical transitions. Sr_2MnO_4 is an n-type Mott insulator and its conduction band is composed of nearly degenerated e_g orbitals $d_{x^2-y^2}$ and $d_{3z^2-r^2}$. The charge modulation spectra for a rectifying Sr_2MnO_4/Nb-doped $SrTiO_3$ junction clearly revealed an optical transition at 1.7 eV, while a linear absorption spectrum is dominated by a transition at 2.0 eV. These are assigned to the transitions from O $2p$ to Mn $d_{3z^2-r^2}$ and to $d_{x^2-y^2}$, respectively. The accumulated charges with a density as high as 8×10^{13} cm^{-2} selectively occupy the nearly localized $d_{3z^2-r^2}$ orbitals that hardly contribute to charge transport.

DOI: 10.1103/PhysRevB.86.125127 PACS number(s): 78.20.−e, 73.20.−r, 73.40.Lq, 78.20.Jq

I. INTRODUCTION

Physical properties of condensed matters are in general governed by the outermost orbital nature. In strongly correlated electron systems, the orbital state mutually couples with the charge, spin, and lattice degrees of freedom, giving rise to versatile collective phenomena as typified by the colossal magnetoresistance in perovskite manganites.[1] Recently heterostructures of correlated electron materials have been found to show emergent transport and magnetic properties that are not present in the constituents, and again the orbital state near the interface is of crucial importance for the novel interface electronic phases.[2–8]

To get insight into the complex electronic phases appearing at the interfaces of correlated electron materials, an interface-sensitive probe to the orbital state is indispensable. The electromodulation spectroscopy is one of the techniques to meet the criteria. This technique is a well-established simple technique for detecting slight changes in the optical properties of materials subjected to an electric field.[9] When rectifying heterojunctions are used, an electric field induces charge modulations confined within the width of the accumulation or depletion layers. Therefore, this technique can selectively detect the change in the interfacial electronic state.[10] This charge modulation spectroscopy has revealed a distinctive feature of the band reconstruction in a Mott insulator under electrostatic doping.[11,12]

In this study we applied this technique to a heterojunction composed of Sr_2MnO_4 and Nb doped $SrTiO_3$ (Nb:STO). Sr_2MnO_4 has a K_2NiF_4 type (layered perovskite) structure and the three d electrons fully occupy the lower Hubbard band comprised of the t_{2g} orbitals, making its ground state an insulating G-type antiferromagnetic Mott insulator.[13,14] In an analogy with $SrMnO_3$, one might expect that Sr_2MnO_4 could be doped with electrons by substituting Sr with tri- or tetravalent ions.[15] In reality, however, even dilute electron doping (or band filling) has not been attained by the chemical substitution because of the very low miscibility of rare-earth ions (R) in $Sr_{2-x}R_xMnO_4$.[16] The electrostatic doping is an alternative way and the heterojunction can give an excellent playground for enabling such a carrier doping. Considering that Nb:STO is an electron-doped wide-gap band insulator, Sr_2MnO_4/Nb:STO can be regarded as an n-N isotype heterojunction. Then, an electron accumulation will occur in the narrower gap material Sr_2MnO_4 and the application of a reverse bias voltage to the junction can invoke further carrier injection to Sr_2MnO_4, similar to the case of Sm_2CuO_4/Nb:STO.[11] Owing to the large dielectric constant of Nb:STO, we can modulate a large amount of interfacial charges,[11,17,18] that is, an additional attractive point of this junction, and is important from the viewpoint of the realization of the Mott transistor.[19,20]

One of the distinctive features of Sr_2MnO_4 from those of Sm_2CuO_4 is the orbital degeneracy in the upper Hubbard band. The remaining orbital degree of freedom in Sr_2MnO_4 plays an important role for the doped carriers. While such a carrier doping process in multiorbital Mott insulators has been widely studied both experimentally and theoretically,[21–23] few have achieved direct observations of the orbital structure by spectroscopic techniques under finely controlled doping levels. In this study we intend to reveal the effect of the orbital degree of freedom on the carrier doping process in Sr_2MnO_4 by the charge modulation spectroscopy. Our result clearly reveals no sign of insulator to metal transition and unveils the energy splitting of empty e_g orbitals caused by the structural anisotropy which can hardly be observed by other experimental techniques. The electrons are doped selectively to the $d_{3z^2-r^2}$ orbital that is localized in nature with its robe extending perpendicular to the two-dimensional MnO_2 sheet.

II. RESULTS AND DISCUSSIONS

A. Sample preparation

Thin films of Sr_2MnO_4 were grown on nondoped and Nb 0.01 wt. % doped $SrTiO_3$ (001) substrates by a pulsed laser deposition technique. It has already been reported that the films of (100) oriented Sr_2MnO_4 were readily fabricated on the (100) plane of $LaSrAlO_4$ in the graphioepitaxy mode.[22] However, the fabrication of a (001) oriented Sr_2MnO_4 films requires more precise control of the growth conditions due to the absence

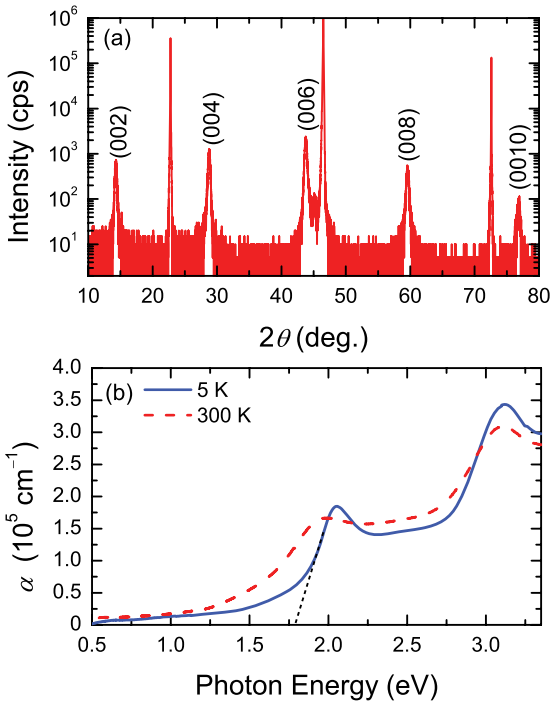

FIG. 1. (Color online) (a) X-ray diffraction pattern of a 30-nm-thick Sr_2MnO_4 film grown on a $SrTiO_3$ substrate. It shows only (0 0 2l) (l = integer) peaks, indicating that the film is in c-axis oriented single crystalline K_2NiF_4 structure. The a- and c-axis lattice constants of the film are 3.83 and 12.41 Å, respectively, which are close to those for a bulk sample (3.79 and 12.49 Å).[13] (b) Linear absorption spectra of the Sr_2MnO_4 film measured at 300 K (dashed line) and 5 K (solid line). The optical band gap of Sr_2MnO_4 film at 5 K is estimated to be 1.8 eV derived from the linear extrapolation (dotted line) of the absorption edge.

of external force to stabilize the layered structure. We tried the deposition at various temperatures and gas pressures, and found that the introduction of oxygen gas causes appearance of impurity phases such as $SrMnO_3$. Single-phase Sr_2MnO_4 films could be obtained at 1070 °C in 1 mTorr pure argon gas pressure. To compensate for the oxygen deficiencies in the substrate and the film generated during the deposition in the reductive growth conditions, the samples were subsequently annealed for 1 h at 450 °C in 760 Torr oxygen atmosphere in the deposition chamber. Figure 1(a) shows an x-ray diffraction pattern of the fabricated film. All the observed peaks can be indexed as (0 0 2l) (l = integer), indicating that the film is grown with its c axis being normal to the film plane without any detectable impurity phases.

Optical absorption spectra of the film grown on nondoped STO are shown in Fig. 1(b). There can be seen two absorption peaks at around 2 and 3.1 eV similar to the optical conductivity spectra for a bulk crystal and (100) oriented film of Sr_2MnO_4 with its electric field parallel to the ab plane.[22,24] These peaks have been assigned to charge-transfer excitation from the O 2p band to the Mn e_g up-spin band and that from the O 2p to the Mn t_{2g} down-spin band, respectively.[24] At 5 K, the lower-energy peak becomes sharper and shows an excitonlike feature, signifying the high crystallinity of the fabricated films.

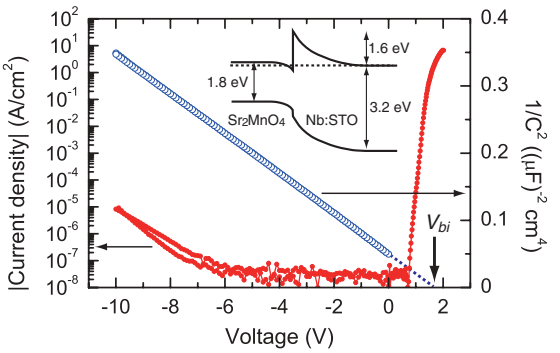

FIG. 2. (Color online) Voltage (V) dependence of current density (J) (filled circles) and inverse square of capacitance (C^{-2}) (open circles) of a Sr_2MnO_4/Nb:$SrTiO_3$ junction measured at 190 K. The J-V curve shows a clear rectification property. The built-in potential qV_{bi} is deduced to be 1.6 eV from the linear extrapolation of the C^{-2}-V line. The inset shows a plausible band structure of this junction in the absence of an external electric field. Due to the notch and spike in the conduction band profile, the electron accumulation takes place in Sr_2MnO_4 under reverse bias.

B. I-V and C-V characteristics of the junction

Hereafter we focus on the junction properties of Sr_2MnO_4/Nb:STO. Figure 2 displays current density-voltage (J-V) and capacitance-voltage (C-V) characteristics of the junction. The J-V curve shows a clear rectification behavior and C^{-2} changes linearly with the bias voltage. Here the forward (reverse) bias is defined as the situation when Sr_2MnO_4 is positively (negatively) biased. The results of J-V and C^{-2}-V indicate the existence of a potential barrier at the interface and a depletion layer in Nb:STO. The linear extrapolation of C^{-2}-V to the voltage axis gives a built-in potential of 1.6 eV. This potential barrier comes from the conduction-band offset as verified by the photocurrent spectroscopy.[25] The possible band structure of this heterojunction deduced from the above results is shown in the inset of Fig. 2. The most important point is the accumulation of electrons in Sr_2MnO_4 which is balanced with ionized donors in the depletion layer of Nb:STO. Applying a reverse bias to this junction can induce further electron accumulation, which we employ for the electromodulation spectroscopy.

C. Electromodulation spectra

Electromodulation spectroscopy was performed by applying a reverse bias ac voltage with a frequency of 570 Hz while irradiating the sample with monochromated light, and the change in the intensity of the transmitted light (ΔT) at the modulation frequency was detected by lock-in technique. The obtained value of $-\Delta T/T$ is equal to $\Delta\alpha d$, where α is the absorption coefficient and d is the effective thickness affected by the charge modulation. Figure 3 displays the electromodulation spectra as well as the absorption spectra of a Sr_2MnO_4 film measured at 190, 90, and 5 K. At all temperatures, the electromodulation spectra show a sign reversal at around 1.5 eV, above (below) which $\Delta\alpha d$ is negative (positive). This is a signature of the spectral weight transfer typically observed when carriers are doped in Mott insulators.[26] The spectral weight transfer is pronounced as the

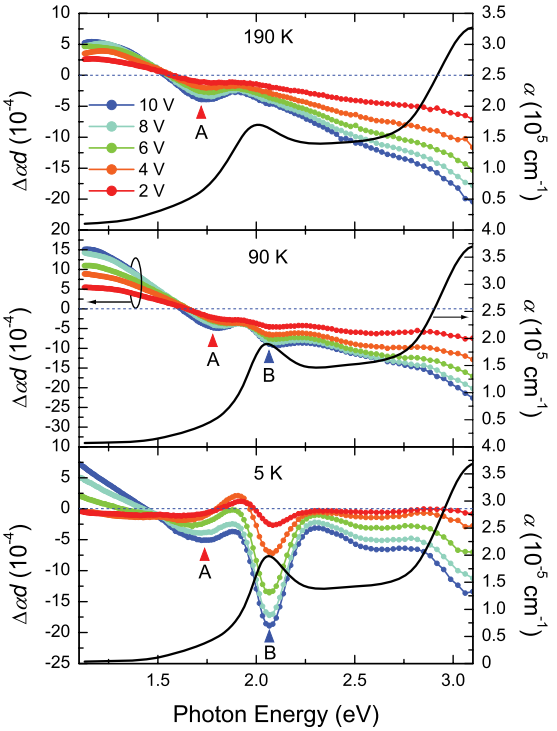

FIG. 3. (Color online) Electromodulation spectra (filled circles) of a Sr_2MnO_4/Nb:$SrTiO_3$ junction (left axis). Measurement temperatures are 190 K (upper panel), 90 K (middle panel), and 5 K (bottom panel). Only one peak at around 1.7 eV can be seen at 190 K (peak A), whereas another peak at around 2 eV emerges by lowering temperature (peak B). Linear absorption spectrum at each temperature is shown by solid line to right axis.

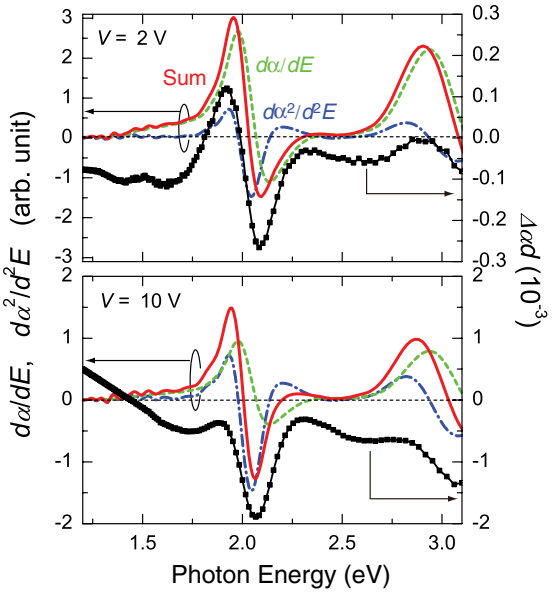

FIG. 4. (Color online) First derivative (dashed line) and second derivative (dashed and dotted line) curves of the absorption spectrum of a Sr_2MnO_4 film at 5 K (left axis). The electromodulation spectra at the same temperature taken at reverse bias voltages of 2 and 10 V are shown to the right axis of upper and lower panels, respectively. The solid line in each panel shows a linear combination of the first and second derivative curves. The relative magnitude between the first and second derivative is determined to fit the peak position and width appearing at around 2 eV.

bias voltage increases, meaning that more carriers are injected. In addition to the change in this wide-energy range, one can see several negative peaks in the electromodulation spectra. The data taken at 190 K has only one peak at around 1.7 eV which we call peak A. Additional peak appears at around 2 eV at 90 K denoted by peak B, and this peak dominantly evolves at 5 K. While peak B has a close correspondence with the peak observed in the linear absorption spectra, there seems to be no corresponding absorption peak for peak A.

We first discuss the origins of peak B appearing at low temperatures. In Fig. 4 are shown first derivative (dashed line) and second derivative (dashed and dotted line) curves of the absorption spectrum as well as the electromodulation spectra measured under reverse bias voltages of 2 (upper panel) and 10 V (lower panel) taken at 5 K. By making linear combinations of the first and second derivative curves (solid lines in Fig. 4), the electromodulation spectra can be well reproduced except for the contributions from peak A and the wide-energy range spectral weight transfer. Here we determine the relative magnitude between the first and second derivatives so that the peak positions coincide with those in the electromodulation spectra at around 2 eV. As can be seen, the first derivative is dominant at $V = 2$ V, while the contribution from the second derivative grows up at $V = 10$ V. This result indicates that an external electric field causes a shift of the absorption peak to a lower energy when the field is small, and gradually induces a peak broadening as increasing the electric field, that is known as the Franz-Keldysh effect.[27–29] These phenomena are often observed in various materials under an external electric field, and is distinct from the charge modulation effect that we discuss below.

Figure 5 shows a schematic band diagram of Sr_2MnO_4. Sr_2MnO_4 has a structural anisotropy, and the Mn-O distance along the c axis (1.976 Å) is longer than that in the ab plane (1.894 Å) according to the structural analysis for a bulk sample.[13] Then, it is plausible that the $d_{3z^2-r^2}$ orbital locates at a lower energy than $d_{x^2-y^2}$. We therefore presume that peaks A and B correspond to the transition from O $2p$ to Mn $d_{3z^2-r^2}$ and to $d_{x^2-y^2}$, respectively. Considering the interatomic overlap integral between the O $2p$ and Mn e_g orbitals within the ab plane of a MnO_6 octahedron, only O p_σ-Mn $d_{x^2-y^2}$ and O p_σ-Mn $d_{3z^2-r^2}$ bonds have nonzero values and the former is $\sqrt{3}$ times larger than the latter as shown in Fig. 6(c).[30] Therefore, the former transition is three times larger in the tight-binding regime and will be dominant in the linear absorption spectrum as depicted in the bottom panel of Fig. 5. This is the reason why only one peak corresponding to peak B was observed in the linear absorption spectra. Once electrons are electrostatically doped, they partially fill the lower-energy band among the two e_g orbitals (i.e., $d_{3z^2-r^2}$). This leads to the breaching of the transition to this orbital without affecting the other transition as depicted in the top panel of Fig. 5. Therefore, the charge modulation spectra show a negative peak due to the reduction of the absorption coefficient at the energy for the O $2p$ to $d_{3z^2-r^2}$ transition (peak A). The magnitude of the energy splitting between the unoccupied two e_g orbitals is then deduced to be 0.3 eV at 190 K.

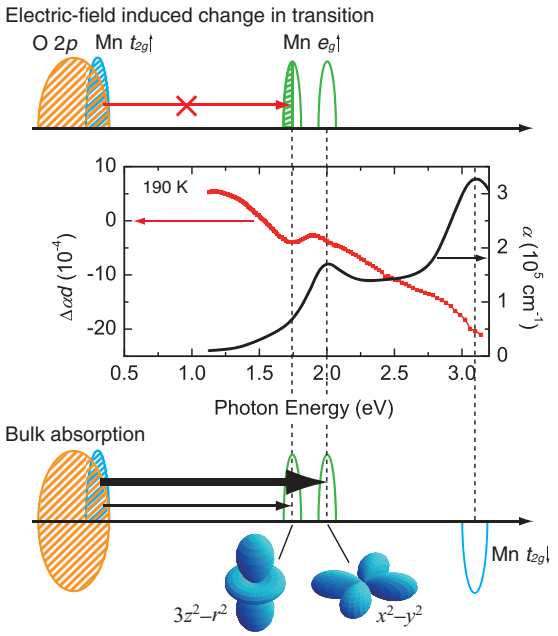

FIG. 5. (Color online) Schematic band diagrams of Sr_2MnO_4 (top and bottom panels) as well as the charge modulation (filled squares) and linear absorption (solid line) spectra measured at 190 K (middle panel). Because of the two-dimensional crystal structure, the originally degenerated two e_g orbitals are split into two bands of $d_{3z^2-r^2}$ and $d_{x^2-y^2}$. Although both the orbitals can contribute to the charge-transfer transition, the transition to $d_{x^2-y^2}$ is stronger and dominant in the linear absorption spectrum as depicted in the bottom panel. Electrostatically doped carriers will occupy the lower $d_{3z^2-r^2}$ band, resulting in the reduction of the transition to this orbital as depicted in the top panel, which appears as the negative peak (peak A) in the electromodulation spectra.

The comparison of the electromodulation spectra for the junction of Sm_2CuO_4 and Sr_2MnO_4 as shown in Fig. 6(a) makes clear the difference in the carrier doping effect between these compounds. The sheet electron densities induced by the reverse bias voltage of 10 V estimated from capacitance measurements are 4.2×10^{13} cm^{-2} for the former and 7.8×10^{13} cm^{-2} for the latter, respectively. In spite of the higher density of electron doping, Sr_2MnO_4 shows much smaller spectral weight transfer in the modulation spectra. In addition, the value of $\Delta\alpha d$ at the lowest photon energy (0.5 eV) is almost zero in Sr_2MnO_4, while Sm_2CuO_4 shows clear positive finite value reminiscent of the metallic conduction. We consider that these differences originate from the character of the orbital occupied by the doped electrons. In Sm_2CuO_4, the conduction band is composed of a $d_{x^2-y^2}$ single orbital as shown in Fig. 6(b) and electrostatically doped electrons can directly contribute to the large electronic reconstruction to make the system metallic. On the contrary, since the electrostatically doped electrons in Sr_2MnO_4 occupy the $d_{3z^2-r^2}$ orbital having more localized nature, they cannot induce a metallic state accompanied by a huge spectral weight transfer. In reality, it is well known that T'-phase layered cuprates including Sm_2CuO_4 can be made metallic or superconducting by the chemical electron doping,[31] but there have been no report on a metallic state in doped Sr_2MnO_4. The present work exemplifies the usefulness of the charge

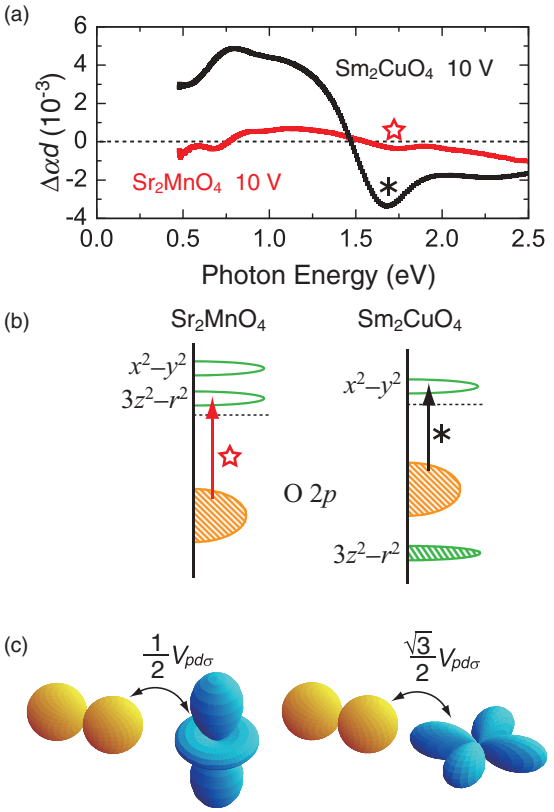

FIG. 6. (Color online) (a) Electromodulation spectra of the Sm_2CuO_4/Nb:$SrTiO_3$ at 300 K (cited from Ref. 11) and Sr_2MnO_4/Nb:$SrTiO_3$ at 190 K including the lower energy part (0.5–1.1 eV). The oscillatory behavior observed in the low-energy part of the spectra for the latter junction is due to the interference of multireflected light in the depletion layer of Nb:$SrTiO_3$. The negative peaks apparent in the modulation spectra denoted by a star ($\star$) and an asterisk ($*$) are the optical transitions in Sr_2MnO_4 and Sm_2CuO_4, respectively, as depicted in (b). (c) Interatomic overlap integral between O $2p\sigma$ and Mn e_g orbitals, where $V_{pd\sigma}$ is defined in Ref. 30.

modulation spectroscopy to get insight into the mechanism of the carrier doping at heterointerfaces of correlated electron materials, especially with multiorbitals.

III. CONCLUSIONS

In conclusion, we performed electromodulation spectroscopy for Sr_2MnO_4/Nb:STO n-N isotype heterojunction. Applying a reverse bias voltage to the junction can modulate the charge accumulation in Sr_2MnO_4. Charge modulation spectra of the junction under reverse bias voltages showed a negative peak at around 1.7 eV, which is lower than the linear absorption peak by 0.3 eV. We consider that the negative peak comes from the transition from the O $2p$ to the Mn $d_{3z^2-r^2}$ orbital, which is undistinguishable in linear optical spectra due to the overlap of the nearby strong transition from the O $2p$ to the Mn $d_{x^2-y^2}$ orbital at around 2.0 eV. The energy difference of 0.3 eV corresponds to the magnitude of the energy splitting between $d_{3z^2-r^2}$ and $d_{x^2-y^2}$ induced by the structural anisotropy in Sr_2MnO_4.

ACKNOWLEDGMENTS

We appreciate A. Sawa, H. Sato, and H. Akoh for device fabrication and fruitful discussions. This work was supported by Japan Society for the Promotion of Science (JSPS) through its "Funding Program for World-Leading Innovative R&D on Science and Technology (FIRST Program)."

*masao.nakamura@riken.jp

[1] Y. Tokura and N. Nagaosa, Science **288**, 462 (2000).
[2] S. Okamoto and A. J. Millis, Nature (London) **428**, 630 (2004).
[3] J. Chakhalian, J. W. Freeland, H.-U. Habermeier, G. Cristiani, G. Khaliullin, M. van Veenendaal, and B. Keimer, Science **318**, 1114 (2007).
[4] G. Jackeli and G. Khaliullin, Phys. Rev. Lett. **101**, 216804 (2008).
[5] M. Salluzzo *et al*., Phys. Rev. Lett. **102**, 166804 (2009).
[6] S. S. A. Seo *et al*., Phys. Rev. Lett. **104**, 036401 (2010).
[7] P. Yu *et al*., Phys. Rev. Lett. **105**, 027201 (2010).
[8] H. Y. Hwang, Y. Iwasa, M. Kawasaki, B. Keimer, N. Nagaosa, and Y. Tokura, Nat. Mater. **11**, 103 (2012).
[9] M. Cardona, *Modulation Spectroscopy* (Academic, New York, 1969).
[10] A. Frova, P. Handler, F. A. Germand, and D. E. Aspnes, Phys. Rev. **145**, 575 (1966).
[11] M. Nakamura, A. Sawa, H. Sato, H. Akoh, M. Kawasaki, and Y. Tokura, Phys. Rev. B **75**, 155103 (2007).
[12] M. M. Qazilbash, Z. Q. Li, V. Podzorov, M. Brehm, F. Keilmann, B. G. Chae, H. T. Kim, and D. N. Basov, Appl. Phys. Lett. **92**, 241906 (2008).
[13] J.-C. Bouloux, J.-L. Soubeyroux, G. L. Flem, and P. Hagenguller, J. Solid State Chem. **38**, 34 (1981).
[14] H. Weng, Y. Kawazoe, X. Wan, and J. Dong, Phys. Rev. B **74**, 205112 (2006).
[15] H. Sakai, S. Ishiwata, D. Okuyama, A. Nakao, H. Nakao, Y. Murakami, Y. Taguchi, and Y. Tokura, Phys. Rev. B **82**, 180409(R) (2010).
[16] S. Larochelle, A. Mehta, L. Lu, P. K. Mang, O. P. Vajk, N. Kaneko, J. W. Lynn, L. Zhou, and M. Greven, Phys. Rev. B **71**, 024435 (2005).
[17] J. Son, S. Rajan, S. Stemmer, and S. J. Allen, J. Appl. Phys. **110**, 084503 (2011).
[18] J. Son, B. Jalan, A. P. Kajdos, L. Balants, S. J. Allen, and S. Stemmer, Appl. Phys. Lett. **99**, 192107 (2011).
[19] D. M. Newns, J. A. Misewich, C. C. Tsuiei, A. Gupta, B. A. Scott, and A. Schrott, Appl. Phys. Lett. **73**, 780 (1998).
[20] C. H. Ahn, J.-M. Triscone, and J. Mannhart, Nature (London) **424**, 1015 (2003).
[21] E. Pavarini, S. Biermann, A. Poteryaev, A. I. Lichtenstein, A. Georges, and O. K. Andersen, Phys. Rev. Lett. **92**, 176403 (2004).
[22] J. Matsuno, Y. Okimoto, M. Kawasaki, and Y. Tokura, Phys. Rev. Lett. **95**, 176404 (2005).
[23] Y. Imai, I. Solovyev, and M. Imada, Phys. Rev. Lett. **95**, 176405 (2005).
[24] Y. S. Lee *et al*., Phys. Rev. B **75**, 144407 (2007).
[25] M. Nakamura, A. Sawa, J. Fujioka, M. Kawasaki, and Y. Tokura, Phys. Rev. B **82**, 201101(R) (2010).
[26] M. B. J. Meinders, H. Eskes, and G. A. Sawatzky, Phys. Rev. B **48**, 3916 (1993).
[27] W. Franz, Z. Naturforsch. Teil A **13**, 484 (1958).
[28] L. V. Keldysh, Sov. Phys. JETP **34**, 788 (1958).
[29] H. I. Ralph, J. Phys. C **1**, 378 (1968).
[30] W. A. Harrison, in *Electronic Structure and the Properties of Solids, The Physics of the Chemical Bond* (Freeman, San Francisco, 1980).
[31] Y. Tokura, H. Takagi, and S. Uchida, Nature (London) **337**, 345 (1989).